



THE UNIVERSITY *of* EDINBURGH

Edinburgh Research Explorer

Improving the ecohydrological and economic efficiency of Small Hydropower Plants with water diversion

Citation for published version:

Razurel, P, Gorla, L, Tron, S, Niayifar, A, Crouzy, B & Perona, P 2018, 'Improving the ecohydrological and economic efficiency of Small Hydropower Plants with water diversion', *Advances in Water Resources*.
<https://doi.org/10.1016/j.advwatres.2018.01.029>

Digital Object Identifier (DOI):

[10.1016/j.advwatres.2018.01.029](https://doi.org/10.1016/j.advwatres.2018.01.029)

Link:

[Link to publication record in Edinburgh Research Explorer](#)

Document Version:

Peer reviewed version

Published In:

Advances in Water Resources

General rights

Copyright for the publications made accessible via the Edinburgh Research Explorer is retained by the author(s) and / or other copyright owners and it is a condition of accessing these publications that users recognise and abide by the legal requirements associated with these rights.

Take down policy

The University of Edinburgh has made every reasonable effort to ensure that Edinburgh Research Explorer content complies with UK legislation. If you believe that the public display of this file breaches copyright please contact openaccess@ed.ac.uk providing details, and we will remove access to the work immediately and investigate your claim.



Improving the ecohydrological and economic efficiency of Small Hydropower Plants with water diversion

Pierre Razurel^a, Lorenzo Gorla^b, Stefania Tron^b, Amin Niayifar^c, Benoît
Crouzy^d, Paolo Perona^{a,*}

^a*School of Engineering, Institute for Infrastructure and Environment, The University of
Edinburgh, Edinburgh, UK*

^b*Group AHEAD, Institute of Environmental Engineering, EPFL-ENAC, Lausanne,
Switzerland*

^c*Stream Biofilm and Ecosystem Research Laboratory, Institute of Environmental
Engineering, EPFL-ENAC, Lausanne, Switzerland*

^d*Federal Office of Meteorology and Climatology, MeteoSwiss, Payerne, Switzerland*

Abstract

Water exploitation for energy production from Small Hydropower Plant (SHP) is increasing despite human pressure on freshwater already being very intense in several countries. Preserving natural rivers thus requires deeper understanding of the global (i.e., ecological and economic) efficiency of flow-diversion practice. In this work, we show that the global efficiency of SHP river intakes can be improved by non-proportional flow-redistribution policies. This innovative dynamic water allocation defines the fraction of water released to the river as a nonlinear function of river runoff. Three swiss SHP case studies are considered to systematically test the global performance of such policies, under both present and future hydroclimatic regimes. The environmental efficiency is plotted versus the economic efficiency showing that efficient solutions align along a (Pareto) frontier, which is entirely formed by non-proportional policies. On the contrary, other commonly used distribution policies generally lie below the Pareto frontier. This confirms the existence of better policies based on non-proportional redistribution, which should be considered in relation to implementation and operational costs. Our results recommend abandoning static (e.g., constant-minimal-flow) policies in favour of non-proportional dynamic ones towards a more sustainable use of the water resource, also considering changing hydroclimatic scenarios.

Keywords: run-of-the-river hydropower plants, environmental benefits,
water allocation policy, dynamic flow releases, hydrological alteration

1. Introduction

Small Hydropower Plants (SHP) are a class of low-capacity (typically lower than 10 MW) energy production power plants often based on either flow diversion from water intakes or run-of-the-river water use concepts. Whenever there is water diversion from the river, and depending on the operational policy, a residual flow is generally released downstream the intake. In part driven by the fear of a Fukushima scenario and in view of limiting carbon emissions from fossil fuel power generation, energy production is turning to renewable sources. Among others, SHP installations are growing although the installed global (i.e., all power plant types) hydropower potential in some countries already exceeds 70% of the feasible potential (e.g., USA and Switzerland, see Figure 1). Some other country, e.g the United Kingdoms, currently uses less than 60% of its potential. Indeed, due to both economic reasons and limitations of technology, sites with lower hydraulic heads or power outputs were not considered as suitable for energy production in the past. This offers some interesting development opportunities for the future provided that environmentally friendly solutions are adopted for further exploitation of freshwater resources. In this work we show how the global (i.e. economic and environmental) performance of flow-diversion practice for feeding SHPs can be improved by engineering a new class of dynamic residual flow policies, and will show this on three real SHP case studies.

We focus on SHPs without significant storage capacity, which withdraw water from an intake installed at a specific river transect, and return it downstream below the power house (Figure 2). Among SHPs, the latter is the scheme with the highest environmental impact in terms of affected riverine corridor length. In the majority of the cases, SHPs also apply residual flow policies set to constant minimal amounts (minimum flow release, henceforth referred to as MFR). Politically simple to define, MFR policies have no specific ecological basis, and their extensive use systematically affected first the morphology and then the ecosystem of river corridors (Poff et al., 2007; Moyle and Mount, 2007). As today's society acknowledges the value of ecosystem services under resource exploitation (Arthington et al., 2006), the classic MFR policy is not sustainable anymore (Poff et al., 2010). Hence, dynamic environmental flow releases mimicking the natural flow regime variability have recently been suggested as preferable (e.g. Basso and Botter

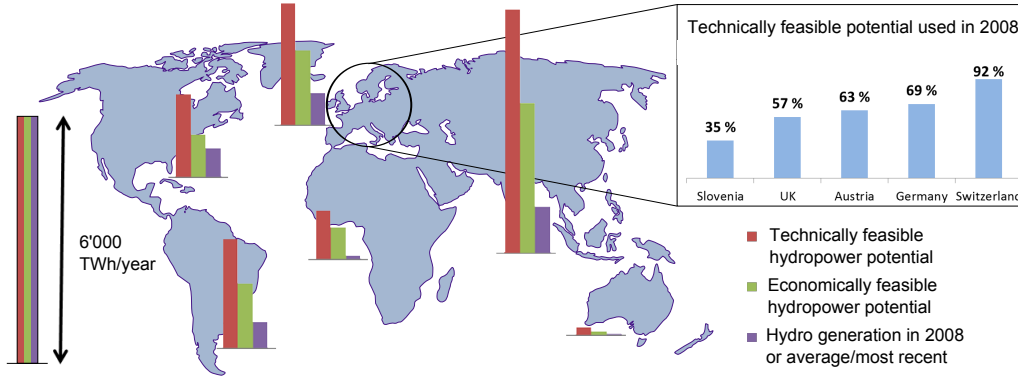


Figure 1: Worldwide consumption of hydropower energy potentials. A detailed view of selected European countries is also provided. Up-to-date (2016) installed vs potential SHP power capacities for Africa (580 vs 12198 MW), Americas (7864 vs 44161 MW), Asia (7231 vs 120588 MW), Europe (18685 vs 32943 MW), Oceania (447 vs 1206 MW) are available in detail from UNIDO (2016).

(2012); Perona et al. (2013)) in order to cope with the ecosystem resilience to perturbations and reduce the risk of critical transitions to different statistical equilibrium states (Scheffer, 2009; Scheffer et al., 2012). Such dynamic redistribution practices (called "proportional" from now on) consist of the release of a certain percentage of the total flow to the environment (e.g., 20%, 30%) while exploiting the remaining fraction up to the plant nominal capacity. Although innovative and beneficial for the environment compared to minimal-flow, proportional policies suffer from the fact that the percentage of redistribution is, by definition, independent of the incoming flow carried by the river.

In order to find more efficient redistribution rules, non-proportional policies have been proposed (Perona et al., 2013; Gorla and Perona, 2013) and their global efficiency preliminary investigated by Gorla (2014) and Razurel et al. (2016). In contrast to proportional policies, the fraction of water released to the environment is defined by a non-linear function which depends on the value of the incoming flow. The conceptual basis of non-proportional redistribution is the paradigm of sustainable development, which recognizes the right of applying limited human pressure to the environment (Arthington et al., 2006). Hence, the more flexible the redistribution rule is, the more efficient the use of water by the riverine ecosystem will be. In this paper we extend the work of Razurel et al. (2016) by first improving the de-

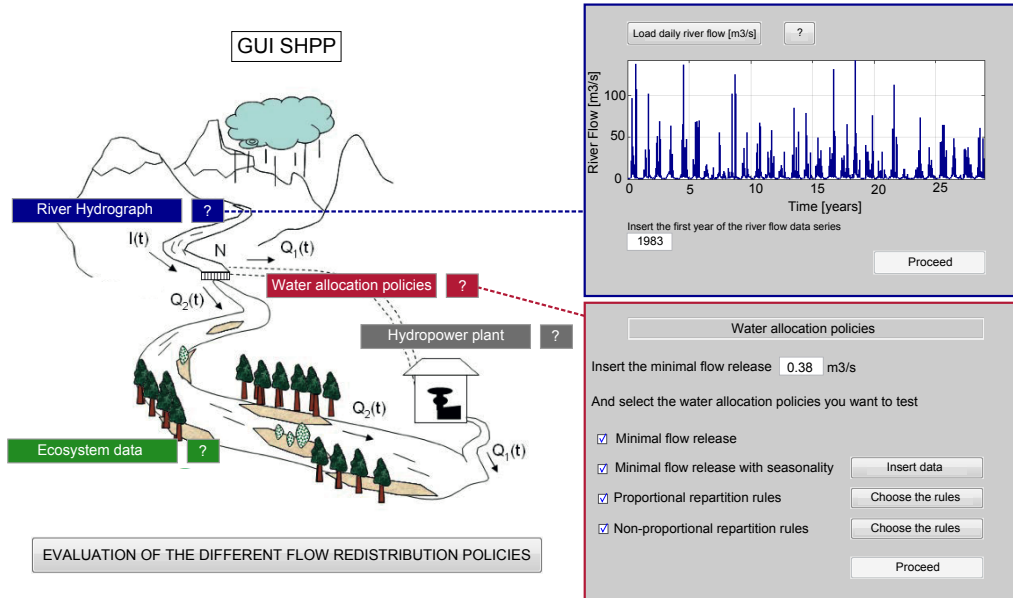


Figure 2: SHP schematics and the corresponding river reach affected by reduced water variability. The two panels on the right show the Graphical User Interface (GUI) developed to perform the numerical simulations. In the top panel the user enters the natural hydrograph used as an input for the model. On the bottom panel, the different water allocation policies simulated by the model can be selected.

90 description of the ecohydrological indicators; second, we numerically simulate
 91 hundreds of thousands of non-proportional policies and show that Pareto
 92 efficient redistribution rules (i.e., the Pareto frontier) are indeed made by
 93 non-proportional policies; third, we perform a sensitivity analysis on the
 94 weight used to compute the ecohydrological indicator. We show the results
 95 for three Swiss case studies also under the effect of changing hydroclimatic
 96 scenarios. Potentially, these policies may be successfully applied to any river
 97 intake structures, which are primarily used to intercept and divert water from
 98 the main stream to serve, as either a storage reservoir or directly for a human
 99 use.

100 2. Methodology and data description

101 2.1. Non-proportional water allocation policies

102 The problem of defining the optimal water allocation for dammed systems
 103 (Castelletti et al., 2007; Soncini-Sessa et al., 1999; Niayifar and Perona, 2017)

clearly simplifies for water intakes with negligible storage capacity. With reference to Figure 2, let us assume that the fraction $Q_1(t)$ of the total incoming flow $I(t)$ at the intake is delivered to the power house. By virtue of the conservation law, the difference

$$Q_2(t) = I(t) - Q_1(t) \quad (1)$$

will be allocated to the riparian ecosystem. The environmental utility for using that water has been shown to be indirectly evaluated by the human use benefit function (Perona et al., 2013). The optimal water allocation can be identified by evaluating which redistribution rule maximizes the global (i.e., economic and environmental) benefits obtained by assigning $Q_1(t)$ to the power house and $Q_2(t)$ to the environment over a reference time frame (Gorla and Perona, 2013).

With the purpose of systematically exploring a large number of water allocation policies representing both proportional and non-proportional redistribution rules, Razurel et al. (2016) introduced a class of nonlinear functions (Gorla, 2014) by modifying the Fermi-Dirac distribution well known in quantum physics (Lifshitz and Landau, 1984). Other ways could have been used to define the non-proportional allocation function but this one has been chosen because it comprises many reasonable redistributions in a simple mathematical function, which is also parsimonious in the number of involved parameters. Thus, the fraction of water that is released to the environment is defined by the following equation:

$$f(x) = \left[1 - M - \frac{Y}{\exp[a(x - b)] + c} \right] (j - i) + i \quad (2)$$

with $M = \frac{A}{A-1}$, $Y = (1 - M)[\exp(-ab) + c]$ and $A = \frac{\exp(-ab)+c}{\exp[a(1-b)]+c}$. This function allows the generation of water allocation policies by varying only few parameters (i, j, a, b), as hereafter described. The parameters i and j are used to set the bound of the Fermi function. The parameter i ranges within $[0;1]$ and represents the fraction of water left in the river at the beginning of the competition ($I = I_{min}$). The parameter j ranges also within $[0;1]$ and correspond to the fraction of the incoming flow rate left in the river at the end of the competition ($I = I_{max}$). Non-proportional allocation starts for an incoming flow rate $I_{min} = Q_{mfr} + Q_{mec}$, where Q_{mfr} represents the minimal flow release and Q_{mec} is the minimum flow required to activate the turbines; below I_{min} , all the water goes to the environment. Initially, a fraction i of

the dimensionless flow $x = \frac{I - I_{min}}{I_{max} - I_{min}}$ above 0 (for $I = I_{min}$) is allocated to the environment as

$$Q_2 = f(x) \cdot (I - I_{min}) + Q_{mfr}, \quad (3)$$

the minimal flow requirement being thus always guaranteed. The competition ends at an incoming flow rate $I_{max} = \frac{Q_N - Q_{mec}}{1-j} + Q_{mfr} + Q_{mec}$, when the nominal power of the turbine is reached at $Q_1 = Q_N$. Therefore, for $I_{min} < Q < I_{max}$ the water is dynamically allocated between the environment and the hydropower plant, depending on the value of the incoming flow I . At the end of the competition, $j < 1$ is the fraction of x left to the environment (see also Razurel et al. (2016) for details). Beyond I_{max} , river discharge exceeding Q_N is allocated to the environment spilling.

When $i = j$ the model generates proportional repartition rules. In this particular case, the quantity of water Q_2 allocated to the river is a fixed percentage (e.g., 10%, 20%) of the water inflow I in addition to the minimal flow requirement. The parameter a allows a variation of the smoothness of the transition between the environmental water allocation i relative to low flows and j relative to high flows (see Figure 3). In the limit of a very large a , one obtains a steep-like transition. Conversely, a small a yields a linear interpolation between i and j . By varying the parameter b , one introduces a change of concavity and controls the position of the inflection point. If the change of concavity is outside the interval $[I_{min}, I_{max}]$, one obtains either a convex or a concave function. Finally, the parameter c gives the overall shape of the curve. Gray curves in Figure 3 show a representative sample of feasible non-proportional water repartition rules given by Equation 2. These were obtained from 36 combinations of a and b , while fixing i and j . Pink curves correspond to the same 36 combinations of a and b , but are obtained by inverting i and j .

2.2. Ecohydrological indicators

River rehabilitation often relies on restoring a more natural flow regime (Petts, 2009; Bartholow, 2010), which suggests that optimal flow releases should be dynamic and show a variability similar to that of the natural flow regime (Poff et al., 1997). We propose to evaluate the environmental performance of the dynamic releases by building a dimensionless synthetic ecohydrological indicator. In particular, this joins the assessment provided by the Indicators of Hydrologic Alteration proposed by Richter et al. (Richter

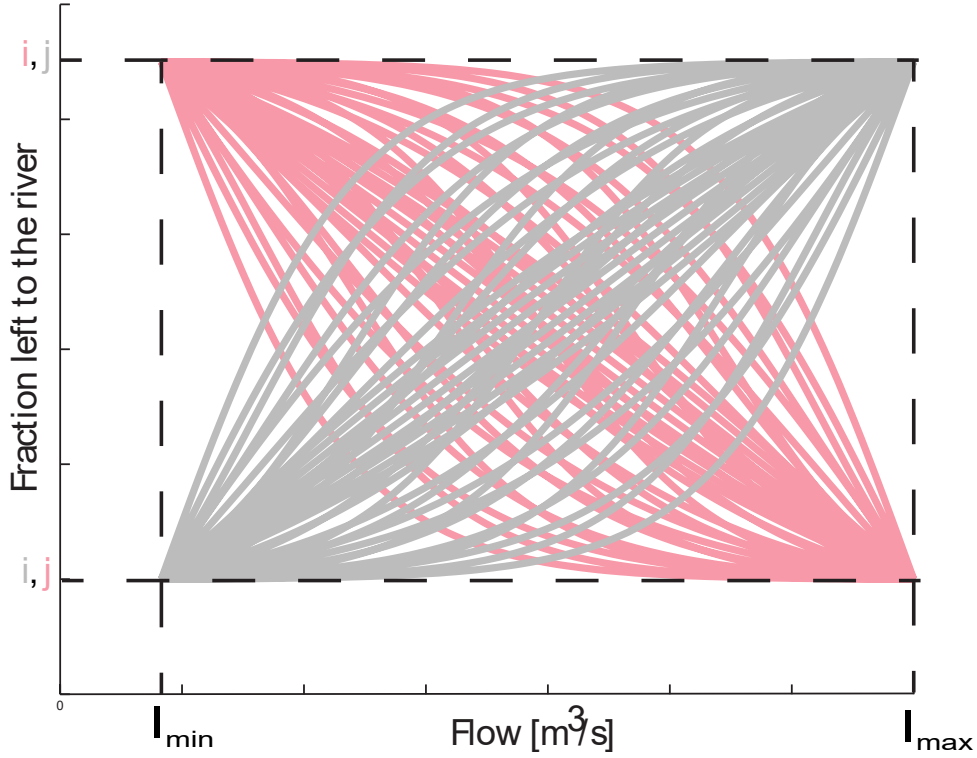


Figure 3: Example of non-proportional repartition rules obtained with the modified Fermi function (Eq. 2). The gray curves show an example of 36 non-proportional functions obtained for different combination of the parameters a and b while i and j are fixed ($i < j$). The pink curves correspond to the same combinations of a and b but parameters i and j are inverted ($i > j$).

et al., 1996) with an evaluation of the habitat availability for fish (Figure 4). Other indicators like the hydro-morphological index of diversity (HMID) developed by Gostner et al. (2013a) exist, and have already been applied to real case studies (Gostner et al., 2013b). Their choice is a valid alternative, which depend, however, on river morphological complexity and general data availability.

The 32 Indicators of Hydrologic Alteration (IHA) proposed by Richter et al. (1996) are an effective attempt to quantify the variability of the natural flow dynamics and deviations from it for altered flow regimes. Coherently with this idea we use the IHAs to minimize the "hydrologic distance" (in terms of *Rate of non Attainment (RnA)* and *Coefficient of Variation (CV)*) between natural conditions and the flow regime resulting from every regu-

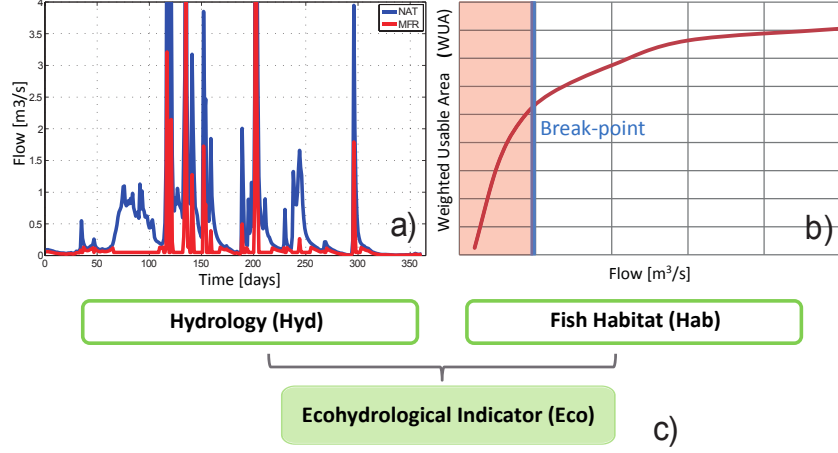


Figure 4: a) Hydrologic differences between the natural flow and environmental releases generated by a classic minimal flow requirement approach (data from the Buseno case study). b) Sketch of the common shape of a Weighted Usable Area (WUA) curve, computed on the basis of surveying and PHABSIM simulations. The break-point generally corresponds to a remarkable change in the slope of the curve. c) Generation of the dimensionless and synthetic ecohydrological indicator *Eco* from hydrologic (*Hvd*) and fish-habitat (*Hab*) information.

lation policy, as detailed in Gorla and Perona (2013). We recall here that the RnA is defined as the fraction of simulated years in which each IHA falls outside a range defined from the natural flow regime (for each IHA). From $RnA(k)$ and $CV(k)$ we compute the indicators $Hyd1_{sim}$ and $Hyd2_{sim}$ by first intra- and subsequently inter-groups of arithmetic means of the IHA (see Gorla and Perona (2013) and Razurel et al. (2016) for details),

$$Hyd1_{sim} = 1 - E \left[(RnA_{sim}(k) - RnA_{nat}(k))^2 \right], \quad (4)$$

$$Hyd2_{sim} = 1 - E \left[(CV_{sim}(k) - CV_{nat}(k))^2 \right], \quad (5)$$

where k refers to each of the 32 IHA.

In addition to hydrologic alteration, habitat availability also plays an important role in species protection. This can be assessed by modelling habitat preference curves generally obtained from river surveys and hydraulic measurements (Milhous et al., 1984a; Maddock, 1999; Bloesch et al., 2005). In the three projects considered in this work, surveys were made on the river reaches impacted by reduced flow with PHABSIM (Physical Habitat Simulation) (Milhous et al., 1984b). Fishing being the main ecosystem of interest

in our case, Weighted Usable Areas (WUA) curves were computed for one dominant fish species, the *brown trout*, discriminating between *juveniles* and *adults* (EcoControl, 2013, 2011, 2012). This method was chosen according to the available data, mainly the hydrograph. Figure 4b shows a qualitative example of the preference curve resulting from PHABSIM method. A common practice to define static threshold, like Q_{mfr} , is to define a breaking point, intended as significant changes of the WUA curve slope, and to consider it as the limit above which a further increase in environmental flow is marginally low. As this method represents a static concept, we improve and extend its use for evaluating dynamic flow releases. We assume that fish stress due to inadequate combination of substrate, water depth and speed, is more relevant when prolonged in time (Payne, 2003). We use the original WUA curves reproducing empirical data and the breaking points recommended in the official project reports in order to identify the threshold (blue line in Figure 4b). Eventually, we quantify the number of consecutive days the environmental release is below the threshold and use this as a proxy for fish habitat conditions.

$Hab1_{sim}$ and $Hab2_{sim}$ thus represent the maximal number of consecutive days, computed over the whole simulation time, characterized by flows under the critical thresholds identified by breakpoints, for juveniles and adults, respectively. Such thresholds were fixed equal to $1.2 [m^3/s]$ for young fish and $0.73 [m^3/s]$ for adults in Buseno, $0.50 [m^3/s]$ for both categories in Cauco, and $0.55 [m^3/s]$ for young fish in Ponte Brolla, where impacts on adults were considered as negligible (EcoControl, 2013, 2011, 2012).

We then aggregate $Hyd1_{sim}$ and $Hyd2_{sim}$ into two hydrological sub-indicators, E_1 and E_2 , bounded between 0 and 1 as

$$E_1 = 1 - \frac{Hyd1_{sim} - Hyd1_{min}}{Hyd1_{max} - Hyd1_{min}}; E_2 = 1 - \frac{Hyd2_{sim} - Hyd2_{min}}{Hyd2_{max} - Hyd2_{min}}. \quad (6)$$

The indicators with subscript *min* and *max* correspond to the scenarios having the minimal and maximal impact on the river, respectively; in this work they correspond to the natural flow regime (no-impact) and to the minimal flow requirement policy.

Similarly, we aggregate $Hab1_{sim}$ and $Hab2_{sim}$ into two fish habitat availability sub-indicators, E_3 and E_4 ,

$$E_3 = 1 - \frac{Hab1_{sim} - Hab1_{min}}{Hab1_{max} - Hab1_{min}}; E_4 = 1 - \frac{Hab2_{sim} - Hab2_{min}}{Hab2_{max} - Hab2_{min}}. \quad (7)$$

The hydrological indicator *Hyd* is calculated by doing the weighted geometric average of the sub-indicators E_1 and E_2 ,

$$Hyd = e^{w_1 \cdot \ln E_1 + w_2 \cdot \ln E_2}, \quad (8)$$

where w_1 and $w_2 = 1 - w_1$ are the weighting factors of E_1 and E_2 . The exponential form is used here as a convenient way of representing the weighted geometrical mean.

The fish habitat indicator *Hab* is calculated by doing the weighted geometric average of the sub-indicators E_3 and E_4 ,

$$Hab = e^{w_3 \cdot \ln E_3 + w_4 \cdot \ln E_4}, \quad (9)$$

where w_3 and $w_4 = 1 - w_3$ are the weighting factors of E_3 and E_4 .

The indicators *Hyd* and *Hab* are finally aggregated to calculate the dimensionless synthetic ecohydrological indicator *Eco*,

$$Eco = e^{w_5 \cdot \ln Hyd + w_6 \cdot \ln Hab}, \quad (10)$$

where w_5 and $w_6 = 1 - w_5$ are the weighting factors of *Hyd* and *Hab*.

Weights should be defined case-by-case, on the basis of expert's opinion and considering the status of the specific riparian ecosystem. In this work we chose not to express preferences and weighted all the indicators as equally important in all numerical simulations (Richter et al., 1996, 1997). However, in order to explore how weighting impact the results, we performed a sensitivity analysis for the weighting factor w_5 .

Table 1: List and parameters of the three case studies considered in this work.

Location	Catchment	Head	Turbine type	Q_N	Q_{mfr_1}	Q_{mfr_2}	Power	Energy Production
	$[km^2]$	$[m]$		$[m^3/s]$	$[m^3/s]$	$[m^3/s]$	$[kW]$	$[GWh]$
Buseno	120	66.5	Cross-flow	4.5	0.38	0.60	2340	8.8
Cauco	89	49.9	Cross-flow	3.5	0.315	0.60	1390	5.0
Ponte Brolla	592	39.5	2 x Francis	12	0.55	0.86	1900	13.9

2.3. Case studies

We chose three small hydropower case studies (henceforth denominated Buseno, Cauco, and Ponte Brolla) located in Southern Switzerland, whose details are reported in Tab.1. For the three case studies we compared the effects of the following sub-classes of water allocation policies: (i) scenarios MFR_1 and MFR_2 , representing traditional minimal flow requirement policies with one or two thresholds (the second one is introduced to increase the minimal flow value from April 1st to September 30th), respectively Q_{mfr_1} and Q_{mfr_2} defined in Table 1; (ii) dynamic flow releases, proportional to $I(t)$ (fixed percentages going from 10% to 50% with a step of 5%); (iii) dynamic flow releases, non-proportional to $I(t)$ (flow-dependent, variable percentages as previously described). In particular, the non-proportional water allocation policies were obtained by varying i and j from 0.02 to 0.70 with 0.01 increment, a from 2 to 8 with step equal to 2, b from 0 to 1 with step 1/8, and considering c constant and equal to 1, for a total of 168912 considered alternatives. The minimal flow requirement Q_{mfr_1} was enforced by law and was therefore always guaranteed for each simulated scenarios.

We used 29 years of streamflow data measured by the Swiss Federal Office for the Environment as natural inflows $I(t)$ to evaluate scenarios in the period 1983 – 2011. For Cauco and Ponte Brolla, power plant locations along the river are not the same as the locations from which the historic flow series have been obtained. We therefore transposed streamflows measured at Buseno (<https://www.hydrodaten.admin.ch/fr/2474.html>) and Bignasco (<https://www.hydrodaten.admin.ch/fr/2475.html>) gauging stations using a surface ratio by rescaling them to the respective catchment areas (Dingman and Dingman, 1994; Brutsaert, 2005). The dependence of hydropower production B_1 on river discharge Q_1 was approximated by a 2nd degree polynomial equation $B_1 = m \cdot Q_1^2 + p \cdot Q_1 + q$, with m , p , and q depending on each plant turbine and associated to a fitting law showing a fitting correlation coefficient R^2 larger than 0.9 (see Gorla (2014) for details).

2.4. Climate change impact on streamflow

The effect of climatic changes on water availability for the the periods 2020-49 and 2070-99 has been obtained by considering the emission RCP 6.0 scenario (Flato et al., 2013), which has been extensively applied to project future climate in several alpine regions of Switzerland. In brief, this scenario foresees by the end of the century a mean global increase of Earth surface temperature of about 2.8°C during summer, with a possible range of +1.7

292 to $+4.5^{\circ}\text{C}$ in Alpine Swiss Cantons. The expected winter temperature vari-
 293 ations are approximately 2°C smaller. The projected precipitation regime
 294 is even more uncertain given the present inherent stochasticity of the phe-
 295 nomenon (Brönnimann et al., 2014). Overall, streamflows are expected to
 296 increase in magnitude in the period 2020 – 2049 due to the melting and
 297 shrinking of alpine glaciers. This scenario will progressively move to a nivo-
 298 pluvial flow regime in the period 2070 – 2099 characterized by higher flows
 299 during late winter, early spring time. Those changes are shown in Figure
 300 5. A recent report (Job et al., 2011) describes the evolution of the Gornera
 301 basin (located in Southern Switzerland near the considered catchments) in
 302 response to such changes and to stored ice and snow in the basin. We con-
 303 sidered this scenario as representative for the three basins chosen and based
 304 on that we generated time series of daily streamflow expected for the periods
 305 2020 – 2049 and 2070 – 2099 for each each basin (e.g. see Gorla (2014)).

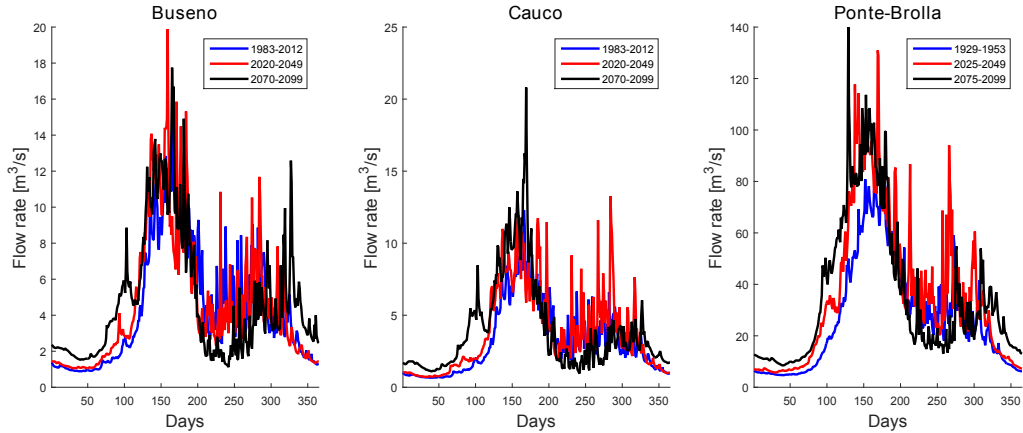


Figure 5: Changes in the mean annual hydrograph for medium and long term under the considered climate scenario RCP 6.0 (Flato et al., 2013) for the three different case studies: Buseno, Cauco and Ponte Brolla.

306 2.5. Development of a Graphical User Interface and Numerical Simulations

307 A Graphical User Interface (GUI) (Figure 2) has been developed using
 308 the software Matlab to facilitate the data treatment and the selection of
 309 the optimal water allocation functions among the different scenarios (non-
 310 proportional, proportional and MFRs repartition rules). For each scenario,
 311 the energy production and the ecohydrological indicators were computed

312 based on the generated flows As a result, the efficiency graph, showing the
 313 mean annual energy produced during the analyzed period versus the ecohy-
 314 drological indicator, was plotted. The Pareto front, representing the ensem-
 315 ble of optimal water allocation scenarios, was identified and enhanced with
 316 a red line in the efficiency plot. More details are provided in Appendix.

317 3. Results

318 3.1. Efficiency plot and selection of optimal scenarios

319 Figure 6 shows the performances of Buseno hydropower plant in terms
 320 of efficiency plot for all the 168912 water repartition rules obtained from
 321 Equation 2. Each gray and pink point of the efficiency plot corresponds to
 322 a non-proportional repartition policy, and can thus be compared to more
 323 classic scenarios, e.g. based on minimal flow requirement and proportional
 324 water allocation policies.

325 As expected, scenario MFR_1 has the highest hydropower production and
 326 the lowest environmental performance. The scenario MFR_2 in Buseno, in
 327 which the minimal release is increased from April 1st to September 30th to
 328 a second fixed threshold, shows a reduction of hydropower production by
 329 3.4% and an increase of ecohydrological indicators by 2.5% with respect to
 330 the performances of MFR_1 . This scenario may be improved by applying
 331 proportional repartition rules. Among these, the one that leaves 10% of the
 332 incoming flow to the environment preserves the energy production of scenario
 333 MFR_2 , while increasing the ecohydrological benefits by 4.7%.

334 However, the benefits obtained with the 10% proportional rule, can still
 335 be improved by moving vertically or horizontally toward the Pareto frontier,
 336 enhancing the ecohydrological indicators and the energy produced, respec-
 337 tively. A notable result is that the Pareto frontier is entirely composed by
 338 non-proportional repartition rules (henceforth referred to as "efficient"). It
 339 is worth recalling here that, at the Pareto frontier, it is not possible to im-
 340 prove a scenario by making an indicator better without making another one
 341 worse. For this power plant, changing a proportional repartition rule with an
 342 efficient one (i.e., that lies on the Pareto frontier) causes a 5% hydropower
 343 production average improvement and a 3% improvement for the ecohydrolog-
 344 ical indicators. These percentages were obtained, with reference to Figure 6,
 345 by moving vertically and horizontally from proportional alternatives towards
 346 points located on the Pareto frontier.

347 Similar results are obtained for Cauco power plant, but not for the one in
 348 Ponte Brolla, as shown in the left-hand side panels of Figure 7. For the latter
 349 case, proportional repartition rules perform already well and the ecohydro-
 350 logical indicator resulting from the simulated alternatives is already high,
 351 thus making the improvement almost negligible, (the potential improvement
 352 of using efficient non-proportional distribution to replace proportional distri-
 353 bution is between 0.0% and 0.1%). This is mainly due to the fact that, in
 354 Ponte Brolla, habitat thresholds (the blue line shown in Figure 4b) turned
 355 out to be lower than Q_{mfr} because of the particular canyoning morphology
 356 of the regulated reach, where a minimal flow release also guarantees fish
 357 survival. Consequently, among the indicators, mainly the hydrologic one
 358 (i.e., *Hyd*) concurred to the definition of the global ecohydrological indicator
 359 *Eco*. This result is consistent with that shown by the sensitivity analysis
 360 performed while changing the weights used to build the ecohydrological indi-
 361 cator (shown ahead). That is, results similar to Ponte Brolla power plant can
 362 be obtained for both Cauco and Buseno in the limit of non considering the
 363 fish habitat availability. A backwards control on sub-indicators and Fermi's
 364 functions (see e.g. subplots in Figure 6) should also be done case-by-case on
 365 the basis of experts opinions in order to check the soundness of interesting
 366 alternatives.

367 3.2. Climate change scenarios

368 Our study shows that a general increase in hydropower production is
 369 foreseen for the periods 2020 – 2049 and 2070 – 2099 for all the three basins
 370 (Figure 7). This right shift toward higher energy production of the efficiency
 371 plot can be explained by an increase of streamflow from 2020 to 2049 and
 372 a seasonal temporal shift of water availability in the period 2070 – 2099,
 373 as predicted by climate models (Figure 5). While the aftermath of glacier
 374 melting in 2020–2049 is obvious as far as energy production is concerned, the
 375 effects of higher winter and spring precipitation expected in the second three
 376 decades requires an explanation. The latter regime sees a flattening of the
 377 current river hydrograph with a strong reduction of the summer maximum.
 378 As a consequence of such redistribution of water availability during the year,
 379 the number of days when turbines can be activated will increase, as the flow
 380 necessary for the turbine to operate, Q_{mec} , will be reached more often. The
 381 impact of climate change on the number of possible operation hours at Q_N
 382 per year is more uncertain, especially if no storage is available.

Table 2: Quantification of the averaged improvements for the alternatives shown in Figure 7. They were obtained by replacing proportional repartition rules with efficient non-proportional ones, improving one indicator at a time.

Foreseen amelioration of non-proportional policies						
Case study	1983-2012		2020-2049		2070-2099	
	Eco	HP	Eco	HP	Eco	HP
Buseno	3.1%	2.4%	4.6%	2.2%	1.8%	1.9%
Cauco	8.6%	1.0%	19.8%	1.0%	22.8%	0.8%
Ponte Brolla	0.1%	2.3%	0.1%	2.6%	0.0%	0.3%

383 The ecological effects of regulation under climate change are complex and
 384 must be analyzed case-by-case. While an exception can be made for Ponte
 385 Brolla, where river morphology always guarantees good habitat availabil-
 386 ity (even under low-flow MFR scenario), both Buseno and Cauco will see a
 387 worsening of both the proportional and constant flow release policies with
 388 respect to non-proportional ones. Table 2 presents the average improvements
 389 obtained by moving from proportional to efficient non-proportional repartitions
 390 located on the Pareto frontier, for the three case studies and the three
 391 time periods. The results show that gains can be obtained through the use of
 392 optimal allocation rules for the three case studies. For Buseno, the potential
 393 gain in ecohydrological indicator goes from 1.8% for the period 1983-2012
 394 to 4.6% for the period 2020-2049. The foreseen amelioration of the energy
 395 production is around 2% for the three considered periods. The most impor-
 396 tant results concerning the ecohydrological indicator are those obtained for
 397 Cauco. Indeed, the foreseen amelioration of the ecohydrological indicator
 398 goes from 8.6% for the period 1983-2012 to 22.8% for the period 2070-2099.
 399 However, the potential gain in energy production is around 1%, which is
 400 lower than the two other case studies on average. Ponte Brolla shows the
 401 lowest gain in ecohydrological indicator, less than 1%, but the improvement
 402 of the energy production for the periods 1983-2012 and 2020-2049 are close
 403 to Buseno. These scenarios are valid assuming that even though the mor-
 404 phology of single river banks is dynamic, average fish habitat conditions in a
 405 river reach will not change over the considered time horizon.

406 4. Discussion

407 4.1. Role of ecohydrological indicator and sensitivity analysis

408 Figure 8 shows the results of the sensitivity analysis performed for the
409 three case studies: (a) Buseno, (b) Cauco and (c) Ponte Brolla. For each of
410 the three plots, the two weighting factors w_1 and w_3 were set to 0.5 while
411 the third factor w_5 was progressively increased from 0 to 1 with a step of
412 0.001. Thus the only parameter that was changed is the weighting of the
413 hydrological indicator Hyd and the fish habitat indicator Hab to compute the
414 final ecohydrological indicator Eco . For each combination of factors, a new
415 efficiency plot is computed. The corresponding average amelioration in both
416 ecohydrological indicator and energy production when replacing proportional
417 rules by non-proportional ones were thus calculated and shown on the Y-axis
418 of the plot.

419 Notably, the sensitivity analysis shows some different results depending
420 on the case study. As far as Buseno (Figure 8 (a)) is concerned, the aver-
421 age improvement of the ecohydrological indicator (red curve) with respect
422 to proportional policies is decreasing when the weighting of the hydrological
423 indicator is bigger than the habitat one, i.e. more weight is given to the
424 hydrological indicator. The gain of energy production (blue curve) starts
425 decreasing when w_5 is above 0.6. This shows that giving a superior weight to
426 the hydrological indicator leads to a reduction in the power production gain.
427 For Cauco (Figure 8 (b)), the same tendency is observed for the environmen-
428 tal gain. However, the variation of the power production as a function of the
429 weighting factor w_5 shows some fluctuations. In contrast to Buseno, no clear
430 tendency is observed. The results for Ponte Brolla (Figure 8 (c)) are differ-
431 ent and the improvements of the power production and the ecohydrological
432 indicator are constant, independently of the value of w_5 . This is explained
433 by the fact that for this specific case, the minimal flow release MFR is always
434 greater than the value of the threshold defined to calculate the fish habitat
435 indicator. Thus, the indicator Hab is always set to the constant maximum
436 value. The order of magnitude of the power production gain is comparable
437 to the other stations but the environmental gain is lower.

438 The absolute value of the ecohydrological indicator has to be interpreted
439 carefully since there is no other previous study applying the same methodol-
440 ogy to combine the hydrological and fish habitat suitability indicators. The
441 indicator has been built to evaluate how far from the natural series each
442 scenario is, a value of 1 corresponding to the natural condition. Thus, we

are more interested in the comparison of the different allocation scenarios and the results we are showing are more focused on the relative gain that may be obtained by using non-proportional policies. We show a method to choose the optimal distribution functions by comparing all the possible distribution methods. The sub-indicators have been chosen according to the available data, being mainly the natural hydrograph and the characteristics of the power plant, but may be improved if more data are available. The allocation rules we are presenting in the paper (non-proportional) have not been implemented yet so there are no empirical data available that allows a comparison between the pre-impact and post-impact systems.

4.2. General considerations and recommendations

Managing water resources to their maximal extent in Alpine countries will necessarily force people to be aware that each unit of energy is generated at some expense of the ecology of the riverine ecosystem. As a consequence, all the feasible measures to improve in efficiency should be taken into consideration together with implementation costs. Some costs are very much country dependent and this aspect is not addressed in this work, being beyond the scope of the work. However, the implementation costs for generating dynamic flow releases are worth a few comments.

This work showed that gains in hydropower production and ecohydrological indicator could be made on average by replacing proportional water allocation policies (today's best practice though not yet widespread) with non-proportional ones located on the Pareto frontier (Table2). Improving both criteria, such increments must be considered as actual win-win solutions. These results are based on testing non-proportional redistribution rules on only three homogeneous SHP case studies limited to the Swiss environment and its socio-economic context. We showed that the potential improvement lies in the wider range of non-proportional repartition rules, with respect to traditional policies. Moreover, Figure 6 demonstrates how classic minimal flow requirement approaches (MFR_1 and MFR_2) can be improved, mainly in term of ecohydrological benefit, by applying non-proportional policies even more than by applying proportional ones (both dynamic). Considering the environment as an independent water user (Perona et al., 2013), with specific needs and features, is thus the key to obtaining efficient environmental flow releases. Such rules will generally result in being non-proportional and flow-dependent. In fact, while the efficiency curve of a turbine does not change throughout the year, the environmental use of water follows seasonal trends.

480 This could easily be added in the model and weighted case-by-case when
481 specific ecological information is available. Increasing the number of case
482 studies would statistically strengthen the results and suggest more general
483 rules to understand which power plants can actually be improved in global
484 performances. This can be challenging to show, particularly because data
485 are often not easily available.

486 In this work, we decided to express the economical indicator as the Energy
487 Production in GWh. This study focuses on Small hydropower plants without
488 storage, hence, this suggests that the optimal strategy would be to always
489 turbine the water diverted according to the chosen allocation rule. However,
490 a further improvement would consist in considering the variability of the
491 electricity market price. This could be made by changing the dimensionless
492 variable x of the Fermi function (Eq. 2) so it does not depend only on the
493 flow rate but also on the market price. Thereby, the value of the produced
494 hydropower production would be optimised (Pereira-Cardenal et al., 2016).

495 Energy provision from renewable sources is a sign of human being respon-
496 sibility, which however requires a strong harmonisation among social, eco-
497 nomic and political parts. The question of how to implement non-proportional
498 flow release rules has not been addressed in this work. However, our present
499 research started to address this problem, particularly looking at suitable hy-
500 draulic infrastructures that may generate Fermi function redistribution rules
501 at zero energy costs (Bernhard and Perona, 2017). This is highly desirable
502 in order to pursue innovation not only from an intelligent technological in-
503 frastructure point of view, but also from a sustainable one.

504 5. Conclusions

505 This work shows a simple and innovative numerical approach for defining
506 sustainable and efficient environmental flow releases in river reaches of SHP
507 without storage. The method has been tested on real data and constraints,
508 and could be adopted as a prompt answer to the actual need to conciliate en-
509 vironmental protection and growth of hydropower production. A convenient
510 class of functions, developed by Gorla (2014) and Razurel et al. (2016), was
511 here comprehensively tested as a practical tool for exploring a representative
512 sample of dynamic flow releases. Such functions provide a direct link between
513 the practice of comparing different environmental flow policies, in particular
514 those using fixed percentages of the incoming flows (proportional) and those
515 with variable splits between diverted and released flows (non-proportional).

516 The Pareto frontier is obtained from the simulated alternatives for each case
517 study and it shows that non-proportional rules are generally more efficient
518 than traditional ones, both proportional and static. It was shown that when
519 applying efficient non-proportional repartition rules for regulating the run
520 of the river hydropower plants, ameliorations in hydropower and ecohydro-
521 logical performances can be attained, with respect to proportional policies.
522 Although the three case studies are located in Switzerland the results vary
523 from one case to another, leading to the conclusion that they depend on the
524 river morphology. Indeed, the canyoning morphology in the case of Ponte
525 Brolla implies that the MFR value is always higher than the threshold given
526 by the WUA curve, which results in a maximum value for the fish habitat
527 suitability indicator. For Cauco, the foreseen amelioration for the ecohy-
528 drological indicator is the most important, it goes from 8.6% for the period
529 1983-2012 to 22.8% for the period 2070-2099 but the gain in energy produc-
530 tion is the lowest (around 1%) in comparison to the two other case studies.
531 Buseno and Ponte Brolla show some similar potential gains in energy pro-
532 duction (around 2%) but for the latter the ecohydrological improvement is
533 almost irrelevant (between 0.0% and 0.1%).

534 **Author contribution**

535 Lorenzo Gorla and Pierre Razurel contributed equally to this work.

536 **Acknowledgements**

537 We thank the Swiss National Science Foundation for funding the project
538 REMEDY (Grant No. *PP00P2_153028/1*), as well as Renato Gaggini of
539 EcoControl SA for openly discussing practical details. This work was written
540 whilst PP visited as academic guest of the Group of Climatology at the
541 Institute of Geography of The University of Bern. The anonymous Reviewers,
542 whose comments helped to improve the quality of manuscript are greatly
543 acknowledged.

544 **Appendix**

545 Graphical User Interface (GUI) (Figure 2) has been developed using
546 the software Matlab to facilitate the data treatment and the selection of
547 the optimal water allocation functions among the different scenarios (non-
548 proportional, proportional and MFRs repartition rules). This tool takes the

549 natural river hydrograph and the hydropower plant features (efficiency func-
550 tion, design flow, etc) as inputs. The desired water allocation policies as well
551 as the ecological threshold can also be set. The user-friendly architecture
552 of the GUI (freely available to any user that wants to reservedly test the
553 performances of his own cases¹) makes the model particularly suitable for
554 stakeholder planning, for water managers operations or for academic pur-
555 poses.

556 Numerical simulations were performed in order to model the different al-
557 location functions. The natural daily flow, $I(t)$, was redistributed between
558 the hydropower plant and the river by simulating Eqs(1-3) according to the
559 selected Fermi function and for the entire time series of $I(t)$. For each sce-
560 nario, the energy production and the ecohydrological indicators were com-
561 puted based on the generated flows Q_1 and Q_2 , respectively. The same pro-
562 cedure was repeated for the whole set of selected Fermi function parameters
563 as well as for the proportional and MFRs repartition rules. As a result, the
564 efficiency graph, showing the mean annual energy produced during the an-
565 alyzed period versus the ecohydrological indicator, was plotted. The Pareto
566 front, representing the ensemble of optimal water allocation scenarios, was
567 identified and enhanced with a red line in the efficiency plot.

568 The simulations to asses the impact of the climate change have been
569 performed in the same way for the three case studies (i.e., Buseno, Cauco
570 and Ponte Brolla). The time series of daily streamflow for the three different
571 time periods (i.e., 2000, 2050 and 2100) have been generated from the current
572 natural data series by applying the trend of the RCP 6.0 scenario described
573 in the previous section 2.4.

574 References

- 575 Arthington, A. H., Bunn, S. E., Poff, N. L., Naiman, R. J., 2006. The chal-
576 lenge of providing environmental flow rules to sustain river ecosystems.
577 Ecological Applications 16 (4), 1311–1318.
- 578 Bartholow, J. M., 2010. Constructing an interdisciplinary flow regime recom-
579 mendation. JAWRA Journal of the American Water Resources Association
580 46 (5), 892–906.

¹free download from <http://www.sccer-soe.ch/research/hydropower/task2.4/> or by simply contacting the authors (PR, PP)

- 581 Basso, S., Botter, G., 2012. Streamflow variability and optimal capacity of
582 run-of-river hydropower plants. *Water Resources Research* 48 (10).
- 583 Bernhard, F. A., Perona, P., 2017. Dynamical behavior and stability analysis
584 of hydromechanical gates. *Journal of Irrigation and Drainage Engineering*
585 143 (9), 04017039.
- 586 Bloesch, J., Schneide, M., Ortlepp, J., 2005. An application of physical habi-
587 tat modelling to quantify ecological flow for the rheinau hydropower plant,
588 river rhine. *Archiv für Hydrobiologie. Supplementband. Large rivers* 16 (1-
589 2), 305–328.
- 590 Brönnimann, S., Appenzeller, C., Croci-Maspoli, M., Fuhrer, J., Grosjean,
591 M., Hohmann, R., Ingold, K., Knutti, R., Liniger, M. A., Raible, C. C.,
592 et al., 2014. Climate change in switzerland: a review of physical, insti-
593 tutional, and political aspects. *Wiley Interdisciplinary Reviews: Climate*
594 *Change* 5 (4), 461–481.
- 595 Brutsaert, W., 2005. *Hydrology: an introduction*. Cambridge University
596 Press.
- 597 Castelletti, A., de Rigo, D., Rizzoli, A. E., Soncini-Sessa, R., Weber, E.,
598 2007. Neuro-dynamic programming for designing water reservoir network
599 management policies. *Control Engineering Practice* 15 (8), 1031–1038.
- 600 Dingman, S. L., Dingman, S. L., 1994. *Physical hydrology*. Vol. 575. Prentice
601 Hall Englewood Cliffs, NJ.
- 602 EcoControl, Dic 2011. Centralina idroelettrica di Cauco. Effetti della cap-
603 tazione sull’ecosistema acquatico della Calancasca (in Italian).
- 604 EcoControl, May 2012. Valutazione dell’ecosistema fluviale e ricadute del
605 progetto sulla fauna ittica (in Italian).
- 606 EcoControl, Mar 2013. Effetti della captazione sull’ecosistema della Calan-
607 casca (in Italian).
- 608 Flato, G., Marotzke, J., Abiodun, B., Braconnot, P., Chou, S. C., Collins,
609 W. J., Cox, P., Driouech, F., Emori, S., Eyring, V., et al., 2013. Climate
610 change 2013: The physical science basis, contribution of working group 1
611 to the fifth assessment report of the intergovernmental panel on climate
612 change. *Climate Change* 2013.

- 613 Gorla, L., 2014. The riparian environment as a non-traditional water user:
614 experimental quantification and modelling for hydropower management.
615 EPFL.
- 616 Gorla, L., Perona, P., 2013. On quantifying ecologically sustainable flow re-
617 leases in a diverted river reach. *Journal of Hydrology* 489 (0), 98 – 107.
- 618 Gostner, W., Alp, M., Schleiss, A. J., Robinson, C. T., 2013a. The hydro-
619 morphological index of diversity: a tool for describing habitat heterogene-
620 ity in river engineering projects. *Hydrobiologia* 712 (1), 43–60.
- 621 Gostner, W., Parasiewicz, P., Schleiss, A., 2013b. A case study on spatial and
622 temporal hydraulic variability in an alpine gravel-bed stream based on the
623 hydromorphological index of diversity. *Ecohydrology* 6 (4), 652–667.
- 624 Job, D., Angehrn, S., Helland, E., Rietmann, D., Schneider, R., Dupraz, C.,
625 Mueller, C., Boogen, N., Spreng, D., Widmer, F., Hänggi, P., Weingartner,
626 R., Haerberli, W., Linsbauer, A., Paul, F., Bosshard, T., Ewen, T., Kot-
627 larski, S., Schär, C., Fankhauser, A., Bobierska, F., Jonas, T., Bauder, A.,
628 Farinotti, D., Usselman, S., Beer, A., Glassey, T., Ludwig, A., Metraux,
629 V., Ossiaa, M., Pralong, M. R., Rickenmann, D., Stähli, M., Turowski, J.,
630 Zappa, M., 2011. Auswirkungen der Klimaänderung auf die Wasserkraft-
631 nutzung: Synthesebericht. Vol. 38 of *Beiträge zur Hydrologie der Schweiz*.
632 Schweizerische Gesellschaft für Hydrologie und Limnologie SGHL, Bern.
- 633 Lifshitz, E., Landau, L., 1984. Statistical physics (course of theoretical
634 physics, volume 5).
- 635 Maddock, I., 1999. The importance of physical habitat assessment for evalu-
636 ating river health. *Freshwater biology* 41 (2), 373–391.
- 637 Milhous, R., Wegner, D., Waddle, T., Energy, W., Team, L., Flow, I., Energy,
638 W., Team, L., Energy, W., Team, L., 1984a. User’s guide to the physical
639 habitat simulation system (PHABSIM). Department of the Interior, US
640 Fish and Wildlife Service.
- 641 Milhous, R. T., Wegner, D. L., Waddle, T., 1984b. User’s guide to the physi-
642 cal habitat simulation system (phabism). Tech. rep., US Fish and Wildlife
643 Service.

- 644 Moyle, P. B., Mount, J. F., 2007. Homogenous rivers, homogenous faunas.
645 Proceedings of the National Academy of Sciences 104 (14), 5711–5712.
- 646 Niayifar, A., Perona, P., 2017. Dynamic water allocation policies improve the
647 global efficiency of storage systems. *Advances Water Resources* 104, 55–64.
- 648 Payne, T. R., 2003. The concept of weighed usable area as relative suitability
649 index. In: Proceedings of International IFIM users workshop (CD). pp. 1–
650 5.
- 651 Pereira-Cardenal, S. J., Mo, B., Gjelsvik, A., Riegels, N. D., Arnbjerg-
652 Nielsen, K., Bauer-Gottwein, P., 2016. Joint optimization of regional
653 water-power systems. *Advances in Water Resources* 92, 200–207.
- 654 Perona, P., Dürrenmatt, D. J., Characklis, G. W., 2013. Obtaining natural-
655 like flow releases in diverted river reaches from simple riparian benefit
656 economic models. *Journal of environmental management* 118, 161–169.
- 657 Petts, G. E., 2009. Instream flow science for sustainable river management.
658 *JAWRA Journal of the American Water Resources Association* 45 (5),
659 1071–1086.
- 660 Poff, N. L., Allan, J. D., Bain, M. B., Karr, J. R., Prestegard, K. L.,
661 Richter, B. D., Sparks, R. E., Stromberg, J. C., 1997. The natural flow
662 regime. *BioScience* 47 (11), 769–784.
- 663 Poff, N. L., Olden, J. D., Merritt, D. M., Pepin, D. M., 2007. Homogenization
664 of regional river dynamics by dams and global biodiversity implications.
665 Proceedings of the National Academy of Sciences 104 (14), 5732–5737.
- 666 Poff, N. L., Richter, B. D., Arthington, A. H., Bunn, S. E., Naiman, R. J.,
667 Kendy, E., Acreman, M., Apse, C., Bledsoe, B. P., Freeman, M. C., Hen-
668 riksen, J., Jacobson, R. B., Kennen, J. G., Merritt, J. H., Olden, J. D.,
669 Rogers, K., Tharme, R. E., Warner, A., 2010. The ecological limits of
670 hydrologic alteration (ELOHA): a new framework for developing regional
671 environmental flow standards. *Freshwater Biology* 55 (1), 147–170.
- 672 Razurel, P., Gorla, L., Crouzy, B., Perona, P., 2016. Non-proportional repar-
673 titution rules optimize environmental flows and energy production. *Water*
674 *Resources Management* 30 (1), 207–223.

- 675 Richter, B., Baumgartner, J., Wigington, R., Braun, D., 1997. How much
676 water does a river need? *Freshwater Biology* 37 (1), 231–249.
- 677 Richter, B. D., Baumgartner, J. V., Powell, J., Braun, D. P., 1996. A method
678 for assessing hydrologic alteration within ecosystems. *Conservation Biology*
679 10 (4), 1163–1174.
- 680 Scheffer, M., 2009. *Critical transitions in nature and society*. Princeton Uni-
681 versity Press, Princeton and Oxford.
- 682 Scheffer, M., Carpenter, S., Lenton, T. M., et al., 2012. Anticipating critical
683 transitions. *Science* 338, 344–348.
- 684 Soncini-Sessa, R., Villa, L., Weber, E., Rizzoli, A. E., 1999. Twole: a software
685 tool for planning and management of water reservoir networks. *Hydrolog-
686 ical sciences journal* 44 (4), 619–631.
- 687 UNIDO, 2016. *World small hydropower report 2016*. Tech. rep., Department
688 of Energy at the United Nations Industrial Development Organization.

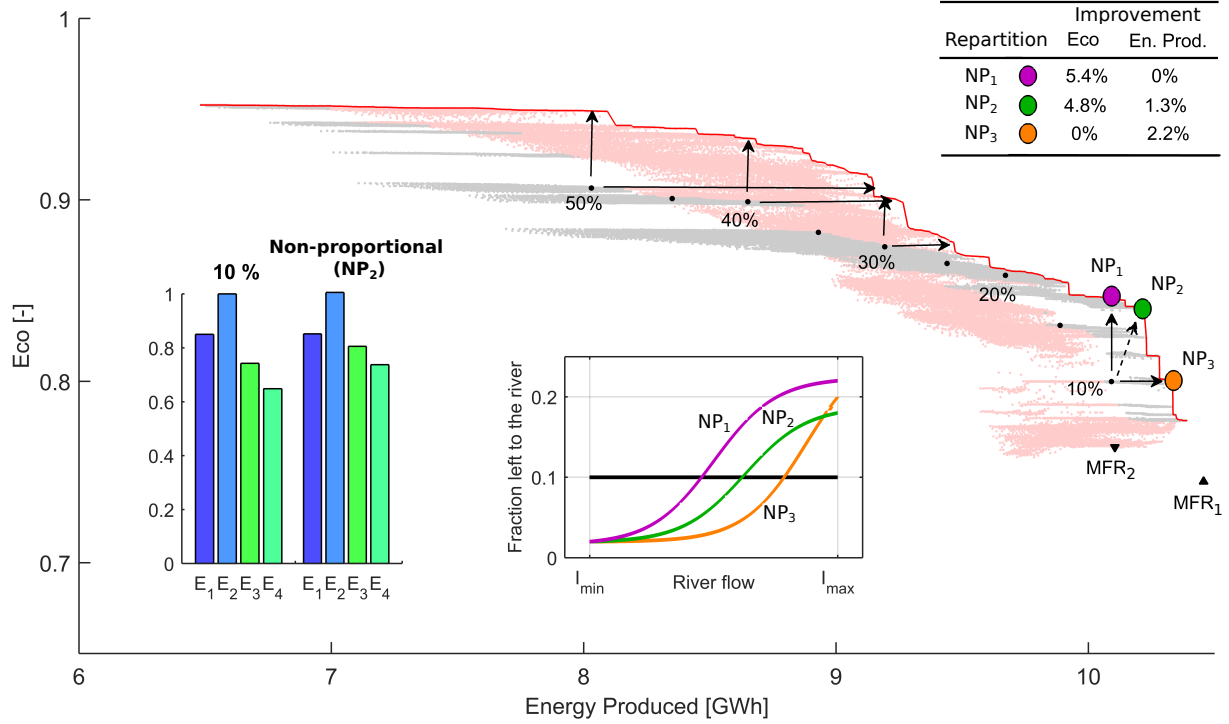


Figure 6: Pareto frontier (red line) and alternatives repartition rules simulated from the 29-years hydrograph (1983-2011) for the Buseno case study. In black are MFR and proportional allocation policies; grey and pink points correspond to non-proportional policies (a subset of these is shown in Figure 3). The black arrows indicate the improvement in term of ecohydrological indicator (vertical ones) and energy produced (horizontal ones) by switching from proportional to non proportional alternatives. The histograms show an example of sub-indicators performances of a proportional (10%) and a non-proportional alternative (green point on the Pareto frontier). The colored curves in the central panel represent the Fermi functions obtained for the three efficient non proportional alternatives to the 10% policy. In the table, the percentages of improvement in ecohydrological indicator and energy production of the non-proportional alternatives NP_1 , NP_2 and NP_3 with respect to the 10% proportional rule are shown.

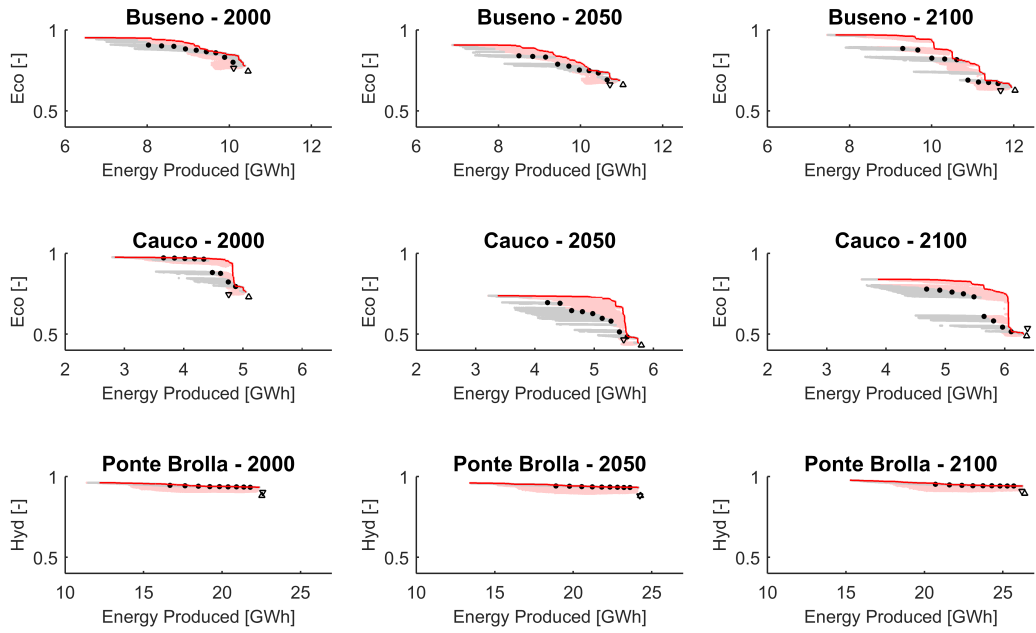


Figure 7: Overview of the alternatives simulated, and the relative Pareto frontiers, for the three case studies under the three considered climatic scenarios (RCP 6.0). Equal weights were assigned for ecohydrological indicators. Colours and symbols are the same of Figure 6.

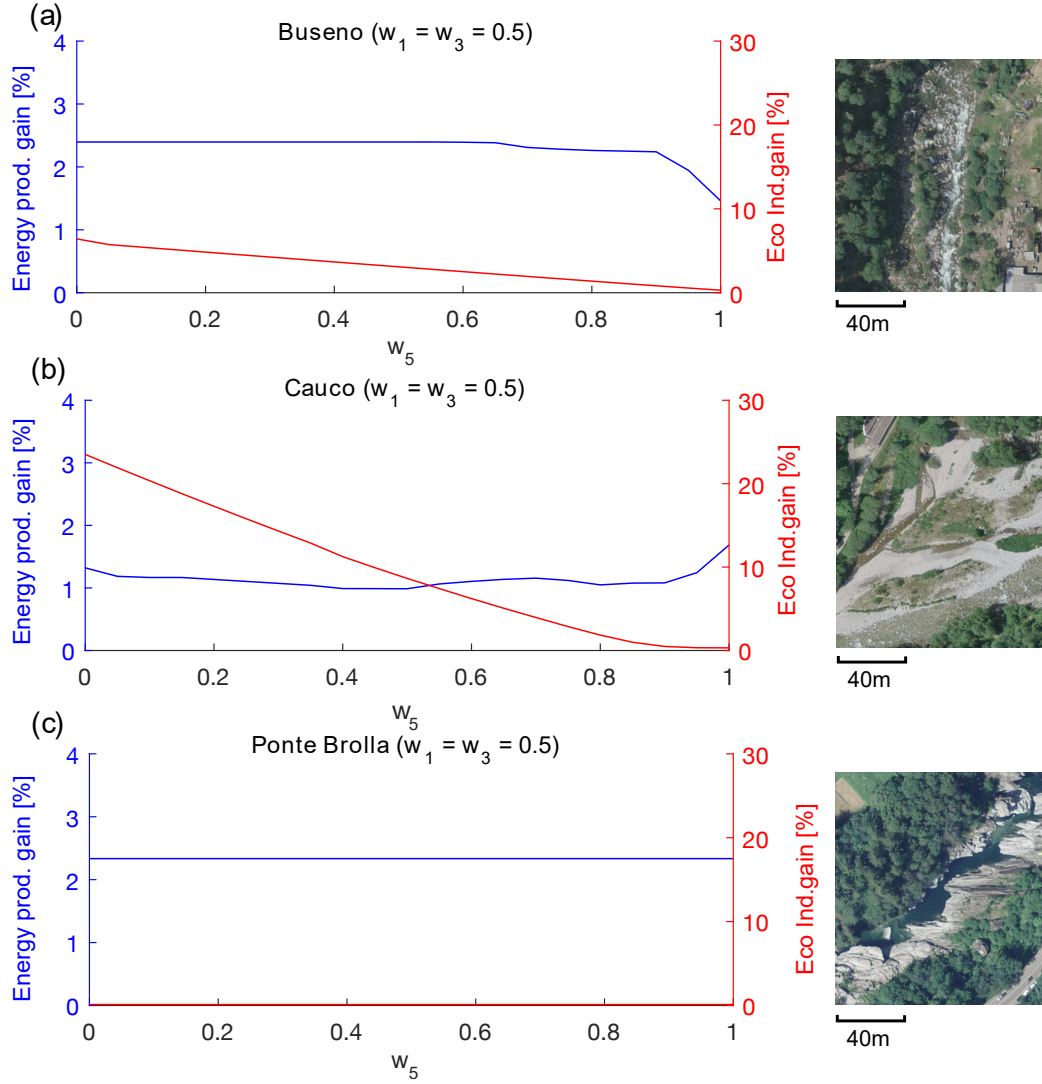


Figure 8: Sensitivity analysis showing the gain in power production (blue curve) and ecohydrological indicator (red curve) with respect to proportional policies and obtained by changing the sub-indicator weighting factors w_1 , w_3 and w_5 as described in Section 2.2. Pictures of the river reach morphologies corresponding to the three case studies are also shown.